

N 7 2 - 1 8 9 1 6

**NASA TECHNICAL
MEMORANDUM**

NASA TM X- 68023

NASA TM X- 68023

**CASE FILE
COPY**

**TEMPERATURE EFFECTS ON THE STRAINRANGE PARTITIONING
APPROACH FOR CREEP-FATIGUE ANALYSIS**

by G. R. Halford, M. H. Hirschberg, and S. S. Manson
Lewis Research Center
Cleveland, Ohio

TECHNICAL PAPER proposed for presentation at
Symposium on Fatigue at Elevated Temperatures sponsored
by the American Society for Testing and Materials
Storrs, Connecticut, June 18-23, 1972

TEMPERATURE EFFECTS ON THE STRAINRANGE PARTITIONING

APPROACH FOR CREEP-FATIGUE ANALYSIS

by G. R. Halford, M. H. Hirschberg, and S. S. Manson

Lewis Research Center
National Aeronautics and Space Administration
Cleveland, Ohio

ABSTRACT

Examination is made of the influence of temperature on the strain-range partitioning approach to creep-fatigue. Results for $2\frac{1}{4}$ Cr-1Mo steel and Type 316 stainless steel show the four partitioned strainrange-life relationships to be temperature insensitive to within a factor of two on cyclic life. Monotonic creep and tensile ductilities were also found to be temperature insensitive to within a factor of two.

The approach provides bounds on cyclic life that can be readily established for any type of inelastic strain cycle. Continuous strain cycling results obtained over a broad range of high temperatures and frequencies are in excellent agreement with bounds provided by the approach. The observed transition from one bound to the other is also in good agreement with the approach.

INTRODUCTION

In a recent paper (Ref. 1), we proposed the Strainrange¹ Partitioning Approach for dealing with creep-fatigue interaction in elevated-temperature, strain-cycling fatigue. The approach holds considerable promise as a practical tool for design purposes and provides a framework for a better understanding of the interaction of creep and plastic deformation during cyclic loading. The basic premise is that cyclic lives

¹Extensive usage of the term, strainrange, warrants the single word spelling.

are governed by the capacity of materials to absorb cyclic inelastic strains. Two types of inelastic strain are considered to be important; time-independent and time-dependent inelastic strain. For simplicity in notation, time-independent inelastic strain will be referred to as plasticity and time-dependent inelastic strain as creep. Plasticity and creep may enter into completely reversed cycles of inelastic strain in a great many different ways. However, four particular combinations appear to have basic significance since they represent extremes in behavior, and because they may be regarded as building blocks for partitioning more complex strain cycles.

Figure 1 shows idealized hysteresis loops that feature the four basic inelastic strain ranges. The widths of these idealized hysteresis loops are defined by:

- $\Delta\epsilon_{pp}$ tensile plastic strain reversed by compressive plastic strain
- $\Delta\epsilon_{cp}$ tensile creep strain reversed by compressive plastic strain
- $\Delta\epsilon_{pc}$ tensile plastic strain reversed by compressive creep strain
- $\Delta\epsilon_{cc}$ tensile creep strain reversed by compressive creep strain

The first letter of the subscript refers to the type of strain (c for creep, p for plasticity) in tension and the second to the type of strain in compression. Procedures for experimentally obtaining the basic partitioned strainrange-cyclic life relationships are presented in Ref. 1.

Preliminary results for $2\frac{1}{4}\text{Cr-1Mo}$ steel presented in Ref. 1 and for Type 316 stainless steel presented in Ref. 2 suggest that the partitioned strainrange-cyclic life relationships for these two engineering alloys (as well as others in their general class) may be insensitive to test temperature. This would hold special significance for three important

reasons, a) the amount of material property data required for analyses could be greatly reduced, b) bounds on cyclic life could be established more readily, even for complex temperature and loading histories, and c) a better understanding of the physical processes of creep-fatigue interaction could result if the cyclic failure criteria are insensitive to temperature - a variable that is normally considered to be of utmost importance to creep-fatigue analysis.

Although temperature may have a small effect on the failure behavior (the partitioned strainrange-life relationships), temperature does have a generally well known, pronounced effect on the flow behavior (the stress-strain, strain rate-temperature relationships). Flow characteristics govern the amount of creep and plasticity encountered during a cycle of inelastic straining. The amounts of creep and plasticity in tension and compression combine to form the partitioned strainranges of the cycle. Since the magnitudes of these strainranges dictate the cyclic life, an analyst interested in predicting life must have a knowledge of both the flow and failure behavior. However, as will be discussed, a detailed knowledge of the flow behavior is not always required, particularly if bounds on cyclic life are sufficient.

The purpose of this paper is to examine some of the effects temperature has on the strainrange partitioning approach. Both the failure behavior and certain aspects of the flow behavior are studied. Implications of the findings are demonstrated using examples which indicate the effects of temperature, frequency, and thermal cycling on the cyclic lives of elevated-temperature, strain-controlled laboratory tests. Experimental results are presented for $2\frac{1}{4}\text{Cr-1Mo}$ steel and for Type 316

stainless steel, each tested over a wide range of temperatures that encompasses their practical use range.

MATERIALS AND EXPERIMENTAL DETAILS

Two materials were used in this study, $2\frac{1}{4}$ Cr-1Mo steel (ASTM A355, Grade P 22) and Type 316 stainless steel. Both were tested in the fully annealed condition. These alloys are typical representatives of a class of high-temperature engineering materials whose mechanical behavior exhibits stability over extended periods of exposure over a broad range of high temperatures. An example of this stability is shown in Table 1 wherein the monotonic tensile (plastic) ductilities and the monotonic rupture (creep) ductilities are tabulated for these materials for several high temperatures. Data for the $2\frac{1}{4}$ Cr-1Mo steel were taken from Ref. 3. Variations in ductility are generally well within a factor of two. As will be pointed out in the RESULTS AND DISCUSSION section, such variations can be considered to be of relatively minor importance in their relation to anticipated cyclic lives.

Specimens for the cyclic studies were of the tubular, hour-glass configuration as described fully in Ref. 4. Heating was either by direct resistance or by an internally positioned silicon carbide heating element. All tests were conducted using closed-loop, servo-controlled, electro-hydraulic equipment. Strains were measured using a diametral extensometer. All strains reported are longitudinal strains calculated from diametral strains. More complete details of the experimental procedures and test equipment can be found in Refs. 1, 4, and 5.

RESULTS AND DISCUSSION

Partitioned Strainrange-Cyclic Life Relationships

The partitioned strainrange-cyclic life relationships for the $2\frac{1}{4}$ Cr-1Mo steel as reported in Ref. 1 are shown in Fig. 2. Additional results generated at 510, 565, and 650 C for this alloy are shown in Table 2, and are plotted in Fig. 2 along with the 595 C baseline data. The partitioned strainrange-cyclic life relationships reported in Refs. 1 and 2 for the Type 316 stainless steel evaluated at 705 C are shown in Fig. 3. New results generated at 595, 650, and 815 C for this alloy are listed in Table 3 and are plotted in Fig. 3 along with the 705 C baseline results.

A few of the tests were conducted with a different temperature in tension than in compression. The two temperatures are listed with the tensile temperature appearing first. Open data symbols are used for the earlier data and closed for the new results. The symbols were chosen to represent the shapes of the hysteresis loops (see Fig. 1 and Ref. 1) of the tests performed. The procedures of Ref. 1 were used to establish the validity of a test result before it was plotted in Figs. 2 and 3.

An overall measure of how well the strainrange partitioning approach can be used to predict creep-fatigue lives for both materials over a spectrum of temperatures is shown in Fig. 4. All of the data generated at the baseline temperature of 595 C for the $2\frac{1}{4}$ Cr-1Mo steel and 705 C for the Type 316 stainless steel are shown by open circles. Data for temperatures both higher and lower are indicated by solid circles. Nearly all of the results fall within a factor of two of the cyclic lives predicted from the baseline results. It is clearly demonstrated that the tempera-

ture dependence of the cyclic lives corresponding to a particular type of inelastic strain is a small one. Hence, for the materials of this investigation, failure data generated at one temperature are applicable over their entire use range of temperatures.

Ductility Considerations

Each of the four independent strainrange-cyclic life relationships may be written in the form,

$$\Delta\epsilon_{ij} = (D_{ij}/N_{ij})^s, \quad ij = \begin{cases} pp \\ cp \\ pc \\ cc \end{cases}$$

where N_{ij} is the cyclic life for the partitioned strainrange $\Delta\epsilon_{ij}$ of interest, and s is the slope of the log-log straight-line relationship. The term D_{ij} may be viewed as a measure of the cyclic strain absorption capacity, or simply the cyclic ductility, for the partitioned strainrange of interest. For a given strainrange, a change in the cyclic ductility will produce an equal change in cyclic life. Hence, nominal variations of, say, a factor of 2 in ductility will influence life to within a factor of about 2.

Extensive experience with plastic strain cycling results at temperatures below the creep range has shown that s is approximately equal to 0.6 for most materials (Ref. 6). Furthermore, the cyclic and the monotonic plastic ductilities have been shown to be approximately equal. Hopefully, similar such correlations can be established between the cyclic ductilities, D_{pp} , D_{cp} , D_{pc} , and D_{cc} and the monotonic creep and plastic ductilities determined in the creep range. However, quantitative correlations should await the availability of additional information on a wide

variety of high-temperature engineering alloys.

A possible correlation is suggested by the present results on $\frac{1}{2}\text{Cr}-1\text{Mo}$ steel and Type 316 stainless steel, since both the monotonic and the cyclic ductilities are insensitive to test temperature to within a factor of two.

Application of Strainrange Partitioning Approach

Some examples of the application of the approach will now be presented that illustrate the implications of having a temperature-independent failure criteria together with temperature-dependent flow behavior. The net influence of temperature on isothermal, continuous strain-cycling lives of tests conducted over a range of temperatures and frequencies is demonstrated using data generated on specimens of Type 316 stainless steel. A brief discussion is also presented regarding the application of the approach to thermal strain cycling problems.

Temperature effect. - Consider a series of constant inelastic strain-range fatigue tests conducted at a constant frequency over a spectrum of isothermal elevated temperatures. At the lower temperatures, the flow behavior is such that the inelastic strain range contains negligible creep. Hence, the inelastic strain range is predominantly $\Delta\epsilon_{pp}$ and the resultant cyclic life is N_{pp} . As the test temperature is raised, time-dependent creep deformation is produced along with the plastic strain. For a "balanced" type of strain cycle, wherein the temperature and strain rates are equal in tension and compression, one would expect an equal amount of creep strain in tension and in compression. Hence, the inelastic strainrange is partitioned by the higher temperature into components of $\Delta\epsilon_{cc}$ and $\Delta\epsilon_{pp}$. The cyclic life will therefore be between the bounding values of N_{cc} and N_{pp} . Finally, at still higher tempera-

tures, the entire inelastic strainrange becomes $\Delta\epsilon_{cc}$ and the ensuing cyclic life is N_{cc} . If the $\Delta\epsilon_{cc} - N_{cc}$ relationship is temperature insensitive, any further increases in isothermal test temperature of the strain cycling tests would not cause the cyclic life to drop below the N_{cc} level.

A series of tests as described above were conducted using Type 316 stainless steel. The inelastic strainrange was chosen nominally equal to 0.0045 with a frequency of 0.02 Hz and a triangular strain-time wave-form. Test temperatures spanned the range from 540 to 870 C. The results of these tests are plotted in Fig. 5 using circular data symbols. Included in Fig. 5 are the partitioned strainrange-cyclic life relationships for $\Delta\epsilon_{cc}$ and $\Delta\epsilon_{pp}$ taken from Fig. 3. These two life lines bound the experimental results. Furthermore, the lowest temperature results lie near the $\Delta\epsilon_{pp} - N_{pp}$ line as expected, and the highest temperature results fall on the $\Delta\epsilon_{cc} - N_{cc}$ line, also as expected. The three dashed lines indicate the cyclic lives expected for cycles with known percentages of $\Delta\epsilon_{cc}$ strain present. For example, test points designated a and b are expected to have had approximately 100% $\Delta\epsilon_{cc}$ (0% $\Delta\epsilon_{pp}$) strain, whereas points d and f fall near the 50% $\Delta\epsilon_{cc}$ (50% $\Delta\epsilon_{pp}$) line.

Frequency effect. - In a series of constant strainrange tests conducted at a fixed temperature over a range of frequencies, one would expect a variation in cyclic life that is somewhat similar to the variation discussed in the previous section. With a sufficiently high frequency of strain cycling, too little time would be available for significant creep deformation to occur. Thus, the inelastic strain in the cycle would be

predominantly plastic strain. The corresponding cyclic life would therefore be N_{pp} . However, if the temperature is in the creep range, a lower frequency would produce creep strain at the expense of plastic strain, and the cyclic life would be lowered, falling between the bounds of N_{pp} and N_{cc} . At extremely low frequencies, one would expect the inelastic strainrange to be composed entirely of completely reversed creep strain, $\Delta\epsilon_{cc}$, with an attendant life of N_{cc} . Further decreases in frequency would not be expected to cause further decreases in cyclic life, since all of the inelastic strain has already been totally absorbed as completely reversed creep strain.

Two series of tests such as just described were conducted on the Type 316 stainless steel. Both were conducted with a nominally constant inelastic strainrange of 0.0045. The series of tests conducted at 705 C covered a frequency variation of nearly four orders of magnitude while the 815 C tests spanned nearly three orders of magnitude. The results of these tests are also shown in Fig. 5 using the square and triangular data symbols. As expected, the highest frequency tests for both temperatures (points i, j, m, and n) failed near the upper bound, N_{pp} , and the lowest frequency tests (points g, h, k, and l) failed near the lower bound, N_{cc} .

The results of the strain cycling tests conducted over a range of temperatures and frequencies are in excellent agreement with the strainrange partitioning approach. The $\Delta\epsilon_{pp} - N_{pp}$ life relationship provides an upper bound on cyclic life while the $\Delta\epsilon_{cc} - N_{cc}$ life relationship provides a lower bound for cycles wherein the type of strain in tension is the same as that in compression. Furthermore, the transition from one

bound to the other is in good qualitative agreement with the approach. The strain cycling lives are functions of temperature and frequency apparently because the flow behavior is highly temperature and rate dependent. The flow behavior governs the amounts of each type of strain-range present, and the temperature and rate insensitive failure criteria in turn govern the cyclic life.

Hence, an important advantage of the approach is that failure data need not be generated over the entire temperature and frequency range. Instead, the life relationships may be determined accurately at a single elevated temperature (with only spot checks conducted at other temperatures) and only the flow behavior determined as a function of temperature and straining rate. Fewer tests are thereby required and their total duration can be significantly reduced.

If bounds on life are adequate, the details of the flow behavior need not be known. However, if the lives for the respective bounds at a selected strainrange are widely separated and a more accurate estimate of cyclic life is required, the flow behavior must be incorporated into the analysis.

Thermal strain cycling. - The strainrange partitioning approach is well suited for application to the complex temperature-strain histories associated with typical thermal fatigue problems. Two aspects of the approach are advantageous, a) the cyclic failure criteria are approximately independent of temperature for certain materials, and b) bounds on cyclic life can be established directly from the strainrange-life relationships.

Consider, for example, a thermal strain cycle wherein a suddenly

applied high-temperature gradient induces compression at the heated surface. Under high stress and temperature, compressive plasticity and creep will be encountered. During the cool-down portion of the cycle, the compressive strain is reversed by tensile strain, which, because of the lower temperature, is predominantly plastic strain (assuming the lower temperature is low enough to preclude creep). In this case, neither $\Delta\epsilon_{cp}$ nor $\Delta\epsilon_{cc}$ type strainranges are present, since there is no tensile creep. Therefore, the only possible components of strainrange are $\Delta\epsilon_{pp}$ and $\Delta\epsilon_{pc}$. In the complex thermal cycle, the plastic and creep strains are accumulated at continuously varying temperatures and strain rates. Since the failure criteria of the strainrange partitioning approach may well be insensitive to these variables, the approach is ideally suited for the analysis of thermal cycling problems. To determine the exact proportions of $\Delta\epsilon_{pp}$ and $\Delta\epsilon_{pc}$ within the cycle would require a detailed and complex analysis of the flow behavior. However, a lower bound on cyclic life could be established directly by simply assuming that all of the inelastic strain is of the $\Delta\epsilon_{pc}$ type.

Other types of thermal strain cycles (for example, wherein the temperature gradient is permitted to disappear at the higher and lower temperatures) may be considered to be composed of $\Delta\epsilon_{cp}$ type strain only. In this case, the lower bound on life could be determined directly from the $\Delta\epsilon_{cp} - N_{cp}$ relationship.

SUMMARY OF RESULTS

A study has been made of the effect of temperature on the strainrange partitioning approach for creep-fatigue analysis. Two high-ductility alloys were investigated, $2\frac{1}{4}$ Cr-1Mo steel and Type 316 stainless steel.

These alloys were taken to be representative of a class of high-temperature materials whose mechanical and metallurgical behavior exhibits stability over extended periods of time over broad ranges of high temperatures. The following major results obtained on these two materials are expected to be applicable to other materials within this class.

1. The partitioned strainrange-cyclic life relationships are insensitive to test temperature to within a factor of two on cyclic life. These life variations are within the range expected considering that the monotonic tensile (plastic) and rupture (creep) ductilities are also insensitive to test temperature to within a factor of two.

2. The strainrange partitioning approach has provided bounds on cyclic life that are in excellent agreement with isothermal, continuous strain-cycling lives for the Type 316 stainless steel over a wide range of temperatures and frequencies. The observed transition from one bound to the other is in good qualitative agreement with the approach.

CONCLUDING REMARKS

For the stable, well-behaved materials studied, we have demonstrated several advantages of the strainrange partitioning approach for creep-fatigue analysis. Since the partitioned strainrange-cyclic life relationships are only a weak function of the elevated test temperature, few data are needed to determine the failure criteria, and bounds on cyclic life can be readily established - even for complex temperature and loading cycles. Since the cyclic lives depend upon the magnitude and types of strains present, rather than on the temperature, stress, or time elapsed to achieve the strains, it appears that strain is the most physically significant of the primary variables in governing the cyclic failure

behavior. The flow behavior, which dictates the amount and type of strain encountered, however, is strongly influenced by the imposed temperature, stress, and time.

Despite the numerous advantages of the strainrange partitioning approach presented in this paper and in Refs. 1 and 2, there are a number of aspects of the problem that still require further attention. These fall into two categories, material behavior and application of the approach. Some of the desirable features of the approach may be lost when dealing with materials whose mechanical properties are unstable with temperature and exposure time. For example, strain-aging phenomena may cause the partitioned strainrange-cyclic life relationships to be somewhat temperature and time dependent. This type of material behavior can still be encompassed by the approach. The drawback is the requirement for more data to characterize the failure behavior as a function of temperature and time. If lower bounds are of primary concern, it may be possible to determine the life relationships for the material in its fully-aged condition, for which the material has the least ductility.

Another material behavior problem area that must be dealt with in its relation to the strainrange partitioning approach is that of corrosion and oxidation. Both may seriously reduce ductility.

The approach, as discussed to-date, requires the inelastic strainrange to be determined explicitly. When the inelastic strainrange is a small fraction of the total strainrange, an accurate determination becomes extremely difficult. Hence, in applying the approach to a practical problem, it may become necessary to add an elastic strainrange term to the partitioned inelastic strainrange to yield the more easily deter-

minable total strainrange. This could be done in a manner analogous to the addition of the elastic and plastic strainrange terms in the Universal Slopes Equation (Ref. 6). Alternatively, when the total strains include a very small inelastic component, elastic theory is applicable and life predictions are better made on the basis of stresses. Extensive analysis by Spera (see, for example, Ref. 7) have demonstrated that thermal fatigue life can be accurately predicted on the basis of time ratios to represent creep effects and cycle ratios to represent fatigue effects in cases where the stresses are nominally within the elastic range.

REFERENCES

1. Manson, S. S., Halford, G. R., and Hirschberg, M. H., "Creep-Fatigue Analysis by Strain-Range Partitioning," Symposium on Design for Elevated Temperature Environment, Am. Soc. Mech. Eng. 1971, pp. 12-24.
2. Manson, S. S., "New Directions in Materials Research Dictated by Stringent Future Requirements," Opening Lecture, International Conference on the Mechanical Behavior of Materials, Kyoto, Japan, Aug., 1971.
3. Jaske, C. E. and Mindlin, H., "Elevated-Temperature Low-Cycle Fatigue Behavior of $2\frac{1}{4}$ Cr-1Mo and 1Cr-1Mo- $\frac{1}{4}$ V Steels," Symposium on $2\frac{1}{4}$ Chromium Molybdenum Steel in Pressure Vessels and Piping, Am. Soc. Mech. Eng. 1971, pp. 137-210.
4. Hirschberg, M. H., "A Low Cycle Fatigue Testing Facility," Manual on Low Cycle Fatigue Testing, ASTM STP 465, Am. Soc. Testing and Mats., 1969, pp. 67-86.

5. Halford, G. R., "Cyclic Creep-Rupture Behavior of Three High-Temperature Alloys," NASA TN D-6309, National Aeronautics and Space Administration, 1971.
6. Manson, S. S., "Fatigue: A Complex Subject - Some Simple Approximations," *Experimental Mech.*, Vol. 5, No. 7, July 1965, pp. 193-226.
7. Spera, D. A., "Experimental Verification of a General Theory for Calculating Thermal Fatigue Life," to be presented at the SYMPOSIUM ON FATIGUE AT ELEVATED TEMPERATURES, Storrs, Conn., 1972.

TABLE 1. - Monotonic tensile (plastic) and rupture (creep) ductilities.

 $2\frac{1}{4}$ Cr-1Mo steel (Ref. 3)

| Test temp., C | Tensile (plastic) | | Rupture (creep) | | Time-to-rupture, hr |
|------------------|-------------------|------------------------|-----------------|------------------------|------------------------|
| | % R.A. | Ductility ^a | % R.A. | Ductility ^a | |
| 510 | 75.0 | 1.38 | 81.1 | 1.67 | 379 |
| | | | 82.6 | 1.75 | 704 |
| | | | 81.8 | 1.70 | 1151 |
| | | | 84.2 | 1.85 | 3285 |
| | | | 85.1 | 1.90 | 4902 |
| 540 | 81.8 | 1.71 | 79.2 | 1.57 | 3 |
| | | | 82.5 | 1.74 | 88 |
| | | | 87.3 | 2.06 | 446 |
| | | | 84.8 | 1.89 | 676 |
| | | | 87.1 | 2.05 | 3013 |
| 565 | 86.1 | 1.96 | 85.5 | 1.93 | 313 |
| | | | 83.6 | 1.81 | 587 |
| | | | 80.2 | 1.62 | 4835 |
| | | | 72.6 | 1.29 | 8014 |
| 595 | 90.7 | 2.36 | 86.2 | 1.98 | 2 |
| | | | 88.4 | 2.15 | 87 |
| 620 | ---- | ---- | 84.7 | 1.88 | 329 |
| 650 | ---- | ---- | 91.7 | 2.48 | 4 |
| | | | 85.9 | 1.96 | 608 |

Type 316 stainless steel

| | | | | | |
|-----|------|------|------|------|------|
| 595 | 63.8 | 1.02 | 40.6 | 0.52 | 301 |
| 705 | ---- | ---- | 69.0 | 1.17 | 10 |
| | | | 74.0 | 1.35 | 31 |
| | | | 66.0 | 1.08 | 111 |
| | | | 58.0 | 0.87 | 362 |
| | | | 77.0 | 1.47 | 848 |
| | | | 73.0 | 1.31 | 1184 |
| 720 | 54.0 | 0.77 | 68.0 | 1.14 | 3408 |
| | | | ---- | ---- | ---- |
| 815 | 65.7 | 1.07 | 72.9 | 1.30 | 116 |

$$^a \text{Ductility} = \ln \frac{100}{100 - \% \text{ R.A.}}$$

TABLE 2. - Creep-fatigue results for $2\frac{1}{4}$ Cr-1Mo steel.

| Spec. no. | Symbol | Temp., C ten/comp | $\Delta\epsilon_{pp}$ | $\Delta\epsilon_{pc}$ | $\Delta\epsilon_{cp}$ | $\Delta\epsilon_{cc}$ | Total inelastic strain range | Observed cyclic life |
|-----------------|--------|-------------------|-----------------------|-----------------------|-----------------------|-----------------------|------------------------------|----------------------|
| 41 | | 510/510 | 0.01990 | ----- | ----- | ----- | 0.01990 | 267 |
| 53 | | 565/565 | .01200 | ----- | ----- | ----- | .01200 | 941 |
| 47 | | 565/565 | .00127 | ----- | ----- | ----- | .00127 | 55 210 |
| 15 | | 650/650 | .00569 | ----- | ----- | ----- | .00569 | 3 234 |
| 30 | | 510/510 | 0.00857 | 0.00338 | ----- | ----- | 0.01195 | 775 |
| 9 | | 650/650 | .01180 | .06140 | ----- | ----- | .07320 | 63 |
| 1 | | 650/650 | .00305 | .01935 | ----- | ----- | .02240 | 180 |
| 25 | | 650/650 | 0.00218 | ----- | 0.00276 | ----- | 0.00494 | 1 350 |
| 10 | | 650/650 | .00247 | ----- | .00311 | ----- | .00558 | 1 950 |
| 26 | | 510/315 | 0.00890 | ----- | 0.01470 | ----- | 0.02360 | 88 |
| 23 ^a | | 510/315 | .00443 | ----- | .00090 | ----- | .00533 | 2 455 |
| 43 | | 510/510 | 0.00889 | ----- | 0.00213 | 0.00520 | 0.01622 | 398 |
| 44 | | 650/650 | .00094 | 0.00240 | ----- | .02470 | .02804 | 100 |

^aNot plotted as $\Delta\epsilon_{cp} - N_{cp}$ result in Fig. 2 since damage due to $\Delta\epsilon_{pp}$ dominated test result.

TABLE 3. - Creep-fatigue results for Type 316 stainless steel.

| Spec. no. | Symbol | Temp., C ten/comp | $\Delta\epsilon_{pp}$ | $\Delta\epsilon_{pc}$ | $\Delta\epsilon_{cp}$ | $\Delta\epsilon_{cc}$ | Total inelastic strain range | Observed cyclic life |
|------------------|--------|-------------------|-----------------------|-----------------------|-----------------------|-----------------------|------------------------------|----------------------|
| 216 | ☒ | 595/595 | 0.01640 | 0.00490 | ----- | ----- | 0.02130 | 262 |
| 217 | ● | 815/815 | .00146 | ----- | ----- | ----- | .00146 | 15 300 |
| 233 | ☐ | 815/815 | 0.00180 | 0.04430 | ----- | ----- | 0.04610 | 51 |
| 225 | ☐ | 815/815 | .00130 | .00540 | ----- | ----- | .00670 | 911 |
| 223 | ☒ | 595/595 | 0.01812 | ----- | 0.00518 | ----- | 0.02330 | 30 |
| 237 | ☐ | 815/815 | .00111 | ----- | .02110 | ----- | .02221 | 17 |
| 218 | ☐ | 815/815 | .00072 | ----- | .00115 | ----- | .00187 | 3 090 |
| 240 | ☒ | 650/315 | 0.00840 | ----- | 0.01200 | ----- | 0.02040 | 22 |
| 239 | ☒ | 650/315 | .00843 | ----- | .00377 | ----- | .01220 | 89 |
| 215 | ☒ | 815/315 | .00445 | ----- | .01425 | ----- | .01870 | 10 |
| 234 | ☒ | 815/315 | .00705 | ----- | .01190 | ----- | .01895 | 25 |
| 222 | ☐ | 815/815 | 0.00222 | ----- | ----- | 0.04593 | 0.04815 | 23 |
| 231 | ☐ | 815/815 | .00108 | ----- | ----- | .00916 | .01024 | 339 |
| 227 | ☐ | 815/815 | .00061 | ----- | ----- | .00209 | .00270 | 3 560 |
| 212 ^a | ● | 815/815 | 0.00395 | ----- | 0.00045 | ----- | 0.00440 | 1 054 |

^aNot plotted as $\Delta\epsilon_{cp} - N_{cp}$ result in Fig. 3 since damage due to $\Delta\epsilon_{pp}$ dominated test result.

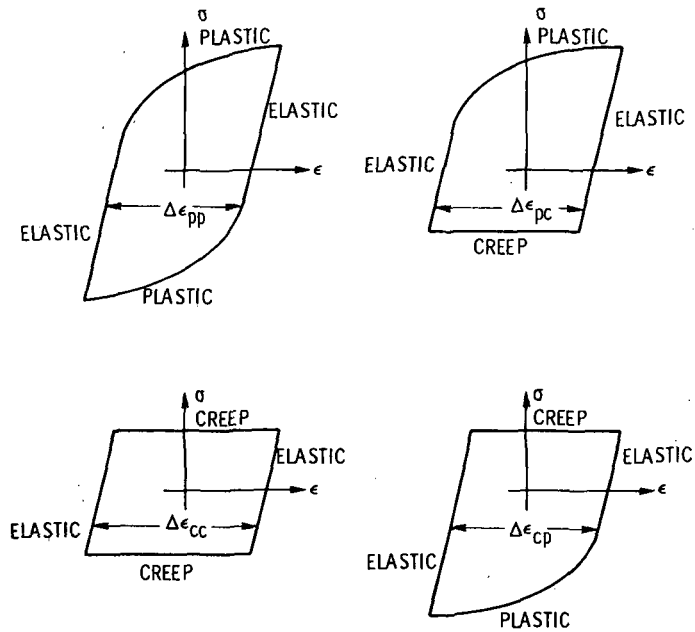


Figure 1. - Idealized hysteresis loops for the four basic types of inelastic strainrange.

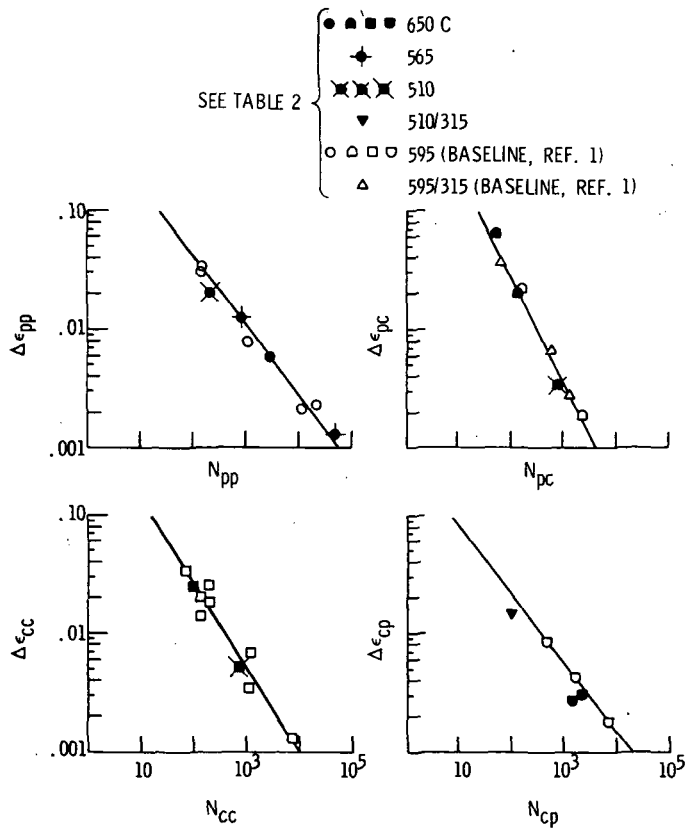


Figure 2. - Partitioned strainrange - life relationships for $2\frac{1}{4}$ CR - 1Mo steel.

E-6829

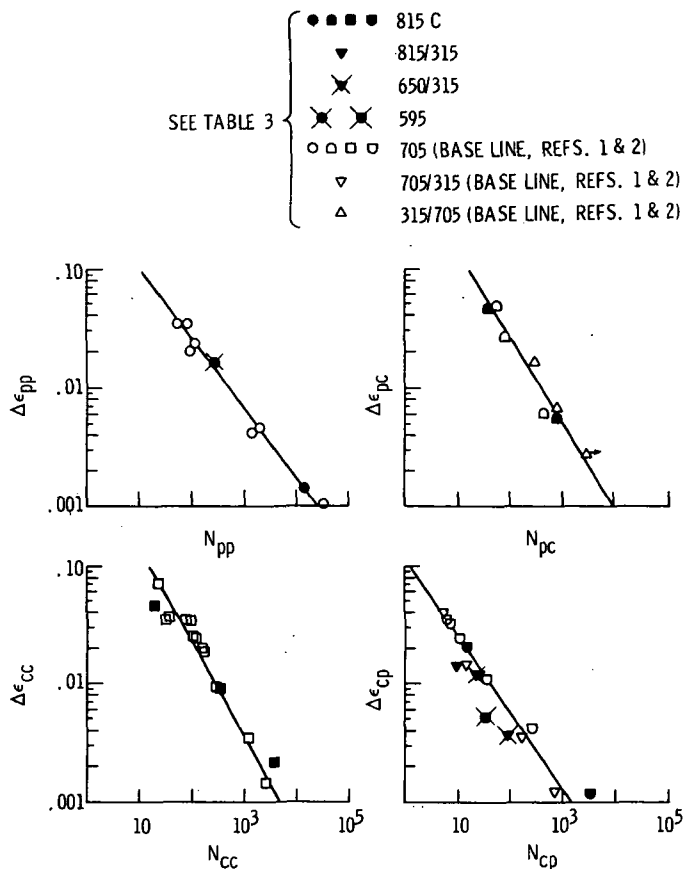


Figure 3. - Partitioned strainrange - life relationships for Type 316 stainless steel.

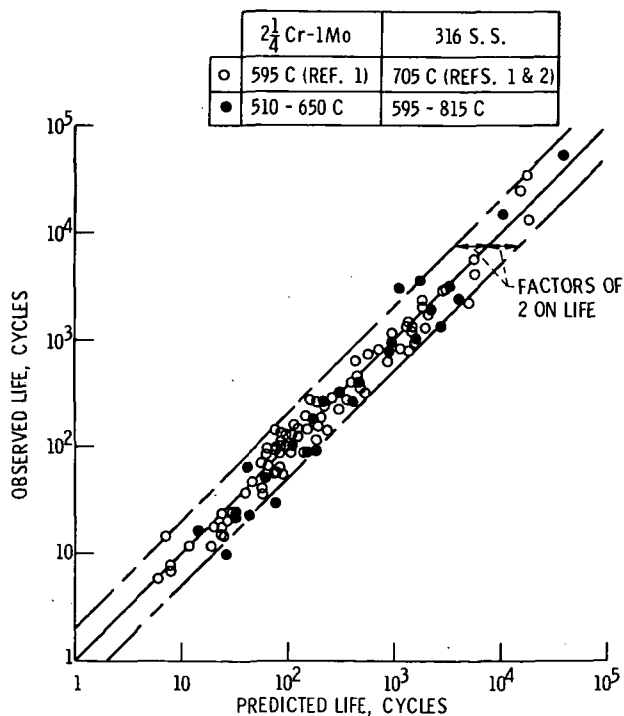


Figure 4. - Comparison of observed and predicted life at different temperatures using strainrange partitioning approach.

TYPE 316 STAINLESS STEEL

| SYMBOL | TEMPERATURE, °C | FREQUENCY, Hz | INELASTIC STRAINRANGE | CYCLES TO FAILURE |
|--------|-----------------|---------------|-----------------------|-------------------|
| a | 870 | 0.02 | 0.00468 | 677 |
| b | 815 | ↓ | .00460 | 730 |
| c | 705 | | .00420 | 2100 |
| d | 650 | | .00400 | 1636 |
| e | 595 | | .00356 | 3507 |
| f | 540 | | .00484 | 1264 |
| g | 705 | | 0.00046 | 0.00510 |
| h | ↓ | .0074 | .00480 | 894 |
| i | | .02 | .00420 | 2100 |
| j | | 2.0 | .00424 | 1700 |
| k | | 815 | 0.003 | 0.00464 |
| l | ↓ | .02 | .00460 | 730 |
| m | | .2 | .00464 | 1950 |
| n | | 2.0 | .00468 | 2350 |

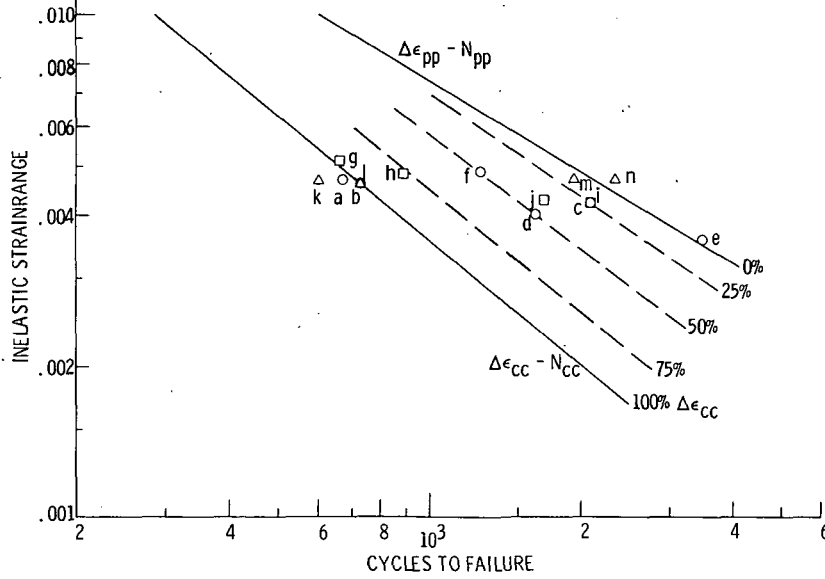


Figure 5. - Application of strainrange partitioning approach to continuous strain cycling results. Temperature and frequency effects are bounded by $\Delta\epsilon_{pp} - N_{pp}$ and $\Delta\epsilon_{cc} - N_{cc}$ relationships.